Available online at www.elixirpublishers.com (Elixir International Journal)

Pollution

Elixir Pollution 108 (2017) 47583-47588

ISSN: 2229-712X

Synthesis and Characterization of Cellulose Coated by Iron Nanoparticles for Treatment some Heavy Metals of Wastewater at 6th October City-Egypt

Yasser A.M. Abdulhady*

Water Treatment and Desalination Unit, Hydrogeochemistry Dept. Desert Research Center, Cairo, P.O.B 11753, EGYPT.

ARTICLE INFO

Article history:

Received: 26 April 2017;

Received in revised form: 28 June 2017;

Accepted: 8 July 2017;

Keywords

Cellulose/iron oxide nano-composites (CIONC),
Heavy metal,
Wastewater treatment,
Removal inorganic pollutants.

ABSTRACT

Small sized iron oxide nanoparticles with were successfully synthesized on the surface of cellulose acetate (CA) by precipitation method. The cellulose acetate were dispersed in deionized water, after that ferric and ferrous chloride was added to this mixture and stirred. After the absorption of iron ions on the surface layer of the fibers, the iron formed was reduced with NaOH by a quick precipitation method. The mean diameter and standard deviation of iron oxide synthesized in cellulose/iron oxide nano-composites (CIONC) were 35 ± 2.42 nm. The prepared nanoparticles were characterized by X-ray diffraction (XRD) analysis, scanning electron microscopy (SEM) and vibrating-sample magnetometer (VSM) and FT-IR. XRD indicated the sole existence of inverse cubic spinel phase of magnetic iron oxide nanoparticles. The cellulose acetate/iron oxide prepared by this method has magnetic properties. The removal efficiency of iron and copper from wastewater by the new synthesized cellulose/ iron oxide nanocomposite after treatment were observed to be 92.96 % and 88.44 %, respectively in synthesized solution. Reduction percent of nitrate and phosphate from wastewater were 86.07% and 91.77 %, respectively. The new prepared cellulose/iron oxide nanocomposite had new physical and chemical characterization by new additives methodology that had high removal efficiency of heavy metals, nitrates and phosphates upon 86-92 % of inorganic pollutants. This research concerned with copper and iron removal from wastewater using magnetic nanoparticles of cellulose/iron oxide.

1. Introduction

Nano-cellulose is prepared by a pretreatment of de-lignified fibers and extraction process. Nano-fibrillated cellulose (NFC) is prepared by mild chemical or enzymatic fiber treatment followed by mechanical processing in which the fibers are disintegrated into fibrils. Cellulose nanocrystals (CNC) are prepared by strong acid hydrolysis of cellulose fibers, which results elimination of undesired area leaving the crystalline part of the fibrils left. Cellulose nanocrystals have the same thickness as NFC, i.e., 4–5 nm thick, but are much shorter, i.e., 100–300 nm. Nanocellulose has unique properties, such as high stiffness, high strength, low thermal expansion coefficient and they are also inert in the contact with human tissue. A fiber composite material is defined as a material containing at least two constituents with different mechanical properties and that both constituents remain separated from each other in the final product. The two constituents are referred to as the matrix and reinforcement, and the properties of the final composite material should be superior to the properties of either constituent alone. Nano-composites, composed of different components, can also be tailored to have strong and interactive properties depending on the selection of the constituting materials. Magnetite particles present a very interesting type of magnetic materials that has attracted intensive interest in recent years due to their potential applications in various fields, such as ferro-fluids, catalysts, high-density magnetic recording media and medical diagnosis [1, 2].

The use of magnetic nanoparticles is related to their super paramagnetic characteristics, higher saturation magnetization, and good biocompatibility. Zhang *et al*. synthesized a new magnetic drug-targeting carrier characterized by a core-shell structure. The carrier is composed of cross-linked dextran grafted with a poly (*N*-isopropyl acrylamide-*co*-*N*,*N*-dimethyl acrylamide) shell and super paramagnetic Fe_3O_4 core [3]. Yuan *et al*., describe a magnetic nanoparticles drug carrier for controlled drug release that responds to the change in external temperature or pH [4, 5]. These carriers simultaneously offer the possibility of imaging the delivery process by magnetic resonance imaging. Researchers have proposed several synthesis methods for preparing Fe_3O_4-NPs, such as micro-emulsions, co-precipitation of an aqueous solution of ferrous and ferric ions by a base and sol–gel method [6], sonochemistry [7], colloidal method [8], non-aqueous route [9], pyrolysis reaction, *etc* [10]. Magnetite (Fe_3O_4) is a common magnetic iron oxide that has a cubic inverse spinel structure with close packed oxygen anions and iron cations occupying interstitial tetrahedral and octahedral sites [11]. Due to its strong magnetic and semiconducting properties, magnetite (Fe_3O_4) is one of the preferred well-known filler materials, which is combined with polymers/nano-composites to be used as magnetic recording media, and in medical applications [12]. Therefore, magnetite has the potential for providing the desired magnetic and electrical properties to the final composite.

Tele: 002 01016941598
E-mail address:Yasser_vip6@hotmail.com

Among the various types of magnetic materials, the magnetic–polymer composites represent a class of functional materials where magnetic NPs are embedded in polymer matrixes. Recently, a considerable number of studies have been done on magnetic–polymer nano-composites such as; PVP-coated Fe_3O_4 [13], Fe_3O_4–chitosan and -Fe_2O_3 NPs [14, 15, 16], tyrosinase biosensor based on Fe_3O_4 NPs–chitosan nanocomposite [17], barium alginate caged Fe_3O_4/C18 magnetic NPs [18], polyaniline-coated nano-Fe_3O_4/carbon nano-tube composite as the protein digestion [19], Fe_3O_4/PPy/P(MAA-co-AAm) tri-layered composite [20], Fe_3O_4-PVA nano-composites [21], polyaniline/nano-Fe_3O_4/composites [22], polymer–Fe_3O_4 nano-composites [23], PEI modified Fe_3O_4/Au NPs [24], alginic acid–Fe_3O_4/nanocomposite [25]. The aim of this work was preparation of new cellulose/iron oxide nanocomposite with modified active sites on the surface of particles. These sites contained functional group on the end of cellulose chains which will attach to pollutants with different types.

2- Materials and Methods

2.1. Chemicals and reagents

All chemical materials used in this study were provided from Merck and Sigma Aldrich Companies.

2.2. Experimental Procedure

2.2.1. Preparation of cellulose/ iron oxide nano-composite

Co-precipitation technique is used to synthesize iron oxide as previously reported with some modifications [26]. Briefly, weight of $FeCl_3 \cdot 6H_2O$ dissolved in 500 ml of distilled water afterwards $FeSO_4 \cdot 7H_2O$ were also dissolved in the mixture and heated to 80 °C, add a definite weight of cellulose acetate powder, then ammonia solution and sodium hydroxide were added drop to wise, and pH of the solution was maintained till to 10.80. The precipitate formed was filtered and washed to remove the impurities of chloride ions. The washed precipitate was drying in vacuum to get the final products.

$$Fe^{2+} + 2Fe^{3+} + 8NH_3 \cdot H_2O \longrightarrow Fe_3O_4\downarrow + 8NH + 4H_2O$$

2.3.2. Sample characterization

FT-IR spectra were measured in a transmission mode on a spectrophotometer (PerkinElmer Spectrum Version 10.03.09) Spectrum Two Detector $LiTa0_3$ was used for separating the solid and liquid during the preparation samples. The samples were pressed pellets of a mixture of the powder with KBr. The micrographs of prepared particles were obtained using a Scanning Electron Microscope using SEM Model Quanta 250 FEG (Field Emission Gun). The XRD pattern of TiO_2 and MNPs was obtained using a X-ray diffractometer Schimadzu model: A PAN analytical X-rays diffraction equipment model Xpert PRO with secondary monochromator, Cu-radiation (λ=1.54A^0) at 50k.v.,40 M.A and scanning speed 0.02^o /sec. Magnetic properties of the particles were assessed with a vibrating-sample magnetometer (VSM, Homade 2 tesla). A magnet (Φ 17.5×20 mm, 5500 O e) was utilized for the collection of magnetic particles**.** Basing on the results of measurements, coercivity, remanence and saturation of samples have been determined, from each powder sample a certain amount of sample has been portioned out, put into another container and weighted. The VSM measurements have been performed on every sample.

2.3.3. Examine adsorbents activity

Batch adsorption studies were performed by mixing MNPs with 50 ml of the synthesized wastewater in a flask. For pH adjustment we used standard 0.1M HCl and 0.1M NaOH solutions.

Put the solution mixture of MNPs with wastewater solution in sonicator for different time. After adsorption reached equilibrium, the adsorbent was conveniently separated via an external magnetic field and the solution was collected for metal concentration measurements. MNPs were washed thoroughly with deionized water to neutrality. The concentrations of metal ions were measured by a plasma-atomic emission spectrometer (ICP-AMS, Optima 3000XL, PerkinElmer) in accordance with the Standard Method. In order to obtain reproducible experimental results, the adsorption experiments were carried out at least 3 times.

2.3.4. Laboratory analyses

The analyses include the determination of EC, TDS, pH. The minor, trace and soluble heavy metals and non metals are total nitrogen, NO^{3-}, PO_4^3, B^{3+}, Al^{3+}, Fe^{3+}, Mn^{2+}, Co^{2+}, Cu^{2+}, Ni^{2+}, Cr^{3+}, Cd^{2+}, Pb^{2+}, and Zn^2.

3. Results and Discussion

3.1. Mechanism of Cellulose/iron nano-composite

$Fe(OH)_2$ and $Fe(OH)_3$ formed at pH > 8 by the hydroxylation of the ferrous and ferric ions. Black precipitation is formed immediately with addition of NH_4OH with drop wise of NaOH. The $FeCl_3$ reacts with NH_4OH and forms FeOOH, which, upon heating, further produce into Fe^{2+} and OH^- ions, which consequently assists in the development of Fe_2O_3 ions according to the chemical reactions. The iron oxide nanoparticles formed in solution with addition of cellulose acetate particles and the morphology of iron oxide nanoparticles is changed and have hydroxyl function group with more reduction efficiency occurred. This nano-composite had more specific functional group and more free electrons in dispersion solution that can increase the reduction percent of removal heavy metals.

3.2 Characterization of the adsorbents

3.2.1. Infrared Spectroscopy (FT-IR)

Figure (1) Absorption peaks at 540 cm^{-1} indicated to the Fe–O vibration related to the magnetite (27). The aliphatic C–H stretching, in 1324 and 1418 cm−1 were due to C–H bending vibrations. (28). The IR band at 1725 cm^{-1} is close to the position of -C=O bending vibrations which indicated to presence of acetate group in cellulose chain. The IR band at 3455 cm^{-1} can be assigned to the stretching modes of surface H_2O molecules or to an envelope of hydrogen-bonded surface OH groups and OH groups of cellulose backbone. The shifted band at 1050 cm^{-1} of Cell-Fe-O vibration related to interaction of iron oxide with the active functional group of acetate group in cellulose backbone. The Fe2+ ions are bonded to 2nd and 3rd hydroxyl groups of cellulose that have been oxidized to keto groups and or carboxylate groups upon treatment with hydrogen peroxide. The peak in this region (1510–1520 cm-1) represents the asymmetrical vibration of O=C-C=O or bi dentate Fe2+ complex such as –C-O-Fe-O-Cengaged in coordinate bond formation (29).

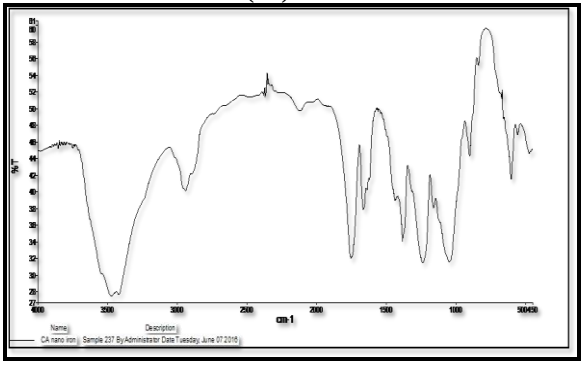

Fig 1. FT-IR spectra of Cellulose/iron nano-composite

The two shoulder peaks formed in the region of 4000–3740 cm-1 are assigned to the cleavage of the primary and secondary hydroxyl groups involved in the coordination complex formation with Fe (30).

3.2.2. X-Ray Diffraction Analysis (XRD)

Figure (2) showed peaks at 2θ of 25.4°,33.2°, 35.3°, 41.4°,49.6° and 54.5° corresponding to the diffractions of crystal faces nano-cell-fibrils, hematite and magnetite spinal structure. The positions and relative intensities of the reflection peak of Fe_3O_4 and Fe_2O_3 MNPs agree with the XRD diffraction peaks of standard Fe_2O_3 samples (31). Sharp peaks showed that Fe_3O_4 and Fe_2O_3 nanoparticles have well crystallized structure and figure showed the sharp band of nano-cell-fibrils

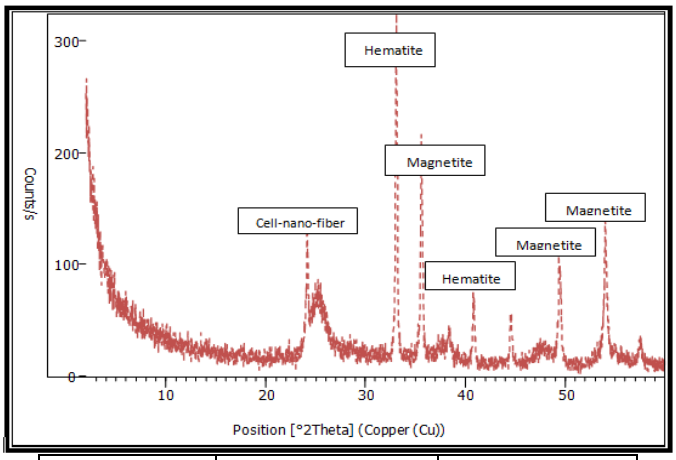

Mineral Name	Chemical Formula	Semi-Quant [%]
Hematite	Fe_2O_3	40
cellulose	Nano Cell Fibrils	25
Magnetite	Fe_3O_4	35

Fig2. XRD- ray of Cellulose/iron nano-composite.

3.2.3. Scanning Electron Micrograph (SEM)

Figure (3) showed the SEM images of cellulose/iron nano-composite which confirmed the cubic and spherical shape of iron oxide nanoparticles of magnetite and hematite onto cellulose fabric which merged with the cross linking of cellulose units. The photo showed the adsorption efficiency of nano iron oxide nanoparticles on the cellulose chains.

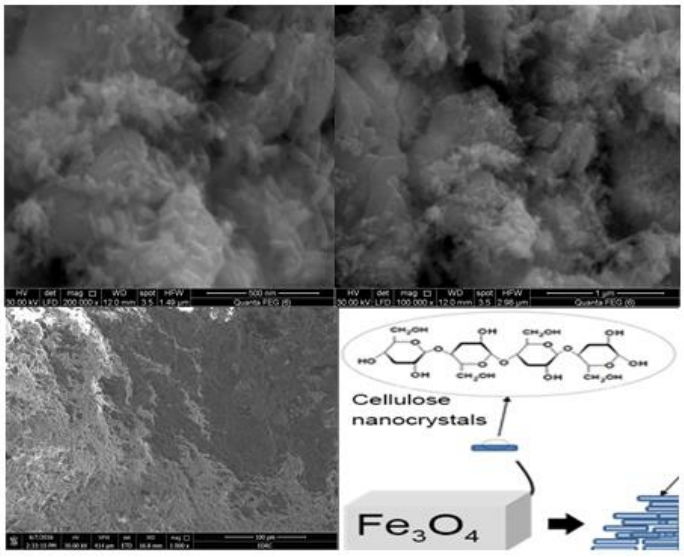

Fig3. Scanning Microscope (SEM) of Cellulose/iron nano-composite

Figure (3) showed that the magnetization curves measured at room temperature for Cellulose/iron oxide nano-composite are showed in Figure 4.

3.2.4. Vibrating Sample Magnetometer (VSM)

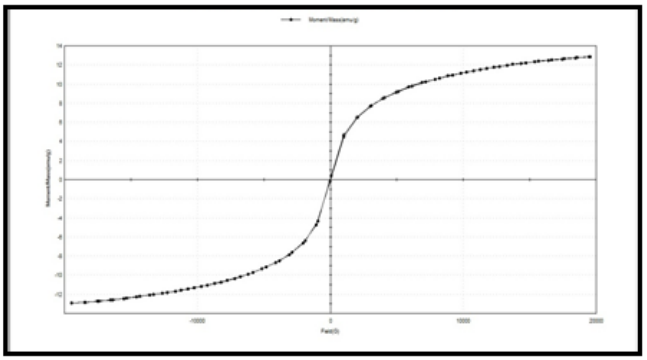

Fig4. Magnetization curves of Cellulose/iron nano-composite.

The low hysteresis in the magnetization for sample showed that produced nanoparticles had paramagnetic strength (32). The saturation magnetization values of Cellulose/iron oxide nano-composite was smaller than the value for the pure magnetite nanoparticles, therefore the saturation magnetization was reduced after addition of Fe_3O_4 and Fe_2O_3 MNPs on cellulose acetate fibrils. The figure indicated that magnetite and hematite nanoparticles were merged in the composite particles, which exhibited no remanence effect from the hysteresis loops at applied magnetic field.

3.3. Effect of Cellulose/iron nano-composite on contaminated wastewater.

3.3.1. Removal of iron and copper ions by Cellulose/iron nano-composite.

Pollutants analyses level in water (inorganic, biological, and organic contaminations) was discussed on the basis of determination with regard to the recommended level of Egyptian standards (1995), Higher committee for water (1995) and WHO (1996). Table (1) showed that the raise level of iron, and copper ions were in permissible standard level. Before treatment the concentration of iron in wastewater was 4.03 ppm as shown in table (1) and it decreased to 0.36 ppm as shown in table (2) after treatment with Cellulose/iron nano-composite. This inhibition indicated that the adsorption efficiency of prepared nanocomposite was (91.06 %) as shown in table (3) and the nano-composite had a nanosized shape with large surface area at optimal condition done. Concentration of copper after treatment decreased to 0.42 ppm as shown in table (2) from 4.96 ppm before treatment as shown in table (1) with reduction percent (91.53 %) table (3).

3.3.2. Removal of nitrate by Cellulose/iron nano-composite

Table (4) showed that the ability of Cellulose/iron nano-composite for removal of nitrate group and nitrate derivatives. The adsorption efficiency (mean reduction percent) of adsorbed nitrate on nanocomposite particles was 86.07 %. The reaction mechanism of adsorption depends on the formation of weak interaction between hydroxyl group and lone pair of electrons on nitrogen atom. This meant that raising of adsorption efficiency of nitrogen compound into nanocomposite and deterioration of nitrogen complex compounds to individuals simple compounds.

3.3.3. Removal of Phosphate content by Cellulose/iron nano-composite

In table (4), the reduction percent of phosphate group adsorbed on nanocomposite particles the mean reduction percent was 91.77 %. The increase of reduction percent caused by the increasing of adsorption and desorption of phosphate group on nanocomposite particles and largest molecular weight of phosphate group.

Table 1. Analysis of heavy metals in ppm before treatment Cellulose/Iron oxide nano-composite

Parameter	Permissible limit	A (Cu)	B (Fe)
	----	8.64 PH	6.20 PH
Aluminum, mg/l	<0.2	1.480	1.130
Boron, mg/l	<0.5	0.020	0.420
Cadmium, mg/l	<0.005	0.002	0.001
Cobalt, mg/l	<0.05	0.010	0.003
Chromium, mg/l	<0.05	0.020	0.020
Copper, mg/l	<0. 5	4.960	0.009
Iron, mg/l	<0.3	0.100	4.030
Manganese, mg/l	<0.5	0.005	0.330
Molybdenum, mg/l	<0.01	0.033	0.005
Nickel, mg/l	<0.1	0.270	0.004
Lead, mg/l	<0.05	0.001	0.030
Vanadium, mg/l	<0.01	0.390	0.010
Zinc, mg/l	<5	1.480	0.450

Table 2. Analysis of heavy metals in ppm after treatment Cellulose/Iron oxide nano-composite

Parameter	Permissible limit	A (Cu)	B (Fe)
	----	8.64 PH	6.20 PH
Aluminum, mg/l	<0.2	1.480	1.130
Boron, mg/l	<0.5	0.020	0.420
Cadmium, mg/l	<0.005	0.002	0.001
Cobalt, mg/l	<0.05	0.010	0.003
Chromium, mg/l	<0.05	0.020	0.020
Copper, mg/l	<0. 5	0.420	0.009
Iron, mg/l	<0.3	0.100	0.366
Manganese, mg/l	<0.5	0.005	0.330
Molybdenum, mg/l	<0.01	0.033	0.005
Nickel, mg/l	<0.1	0.270	0.004
Lead, mg/l	<0.05	0.001	0.030
Vanadium, mg/l	<0.01	0.390	0.010
Zinc, mg/l	<5	1.480	0.450

Table3. Reduction percent of copper & iron before and after treatment by nanocomposite

Serial	Copper/ ppm			Iron/ ppm		
	B.T	**A.T**	R %	**B.T**	**A.T**	R %
A(Cu)	**4.96**	**0.42**	91.53	**0.10**	**0.10**	0.00
B(Fe)	**0.009**	**0.009**	0.00	**4.03**	**0.36**	91.06
S. S	**32.89**	**3.80**	88.44	**64.58**	**4.54**	92.96

S.S: Synthesized solution; B.T: Before treatment; A.T: After treatment; R: Reduction%

Table 4. Reduction percent of nitrate & phosphate before and after treatment by nanocomposite

Serial	NO3-N ppm			PO4-P ppm		
	B.T	**A.T**	**R %**	**B.T**	**A.T**	**R %**
A	64.25	15.23	76.29	58.22	10.10	82.65
B	71.98	12.36	82.82	49.67	13.45	72.92
S.S	40.56	5.65	86.07	60.29	4.96	91.77

S.S: Synthesized solution; B.T: Before treatment; A.T: After treatment; R: Reduction%.

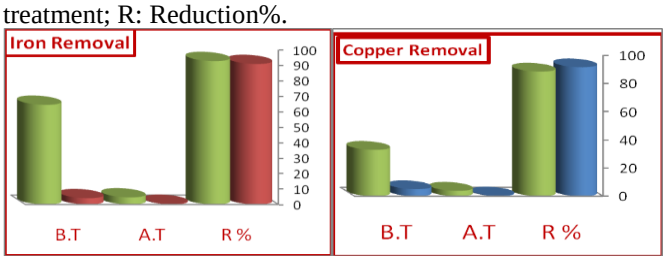

Figure 5. The removal efficiency of copper & iron before and after treatment by nanocomposite

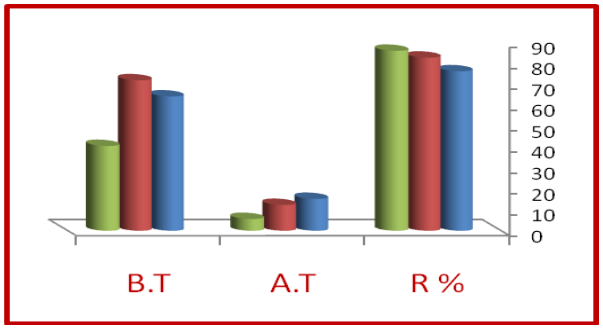

Figure 6. The removal efficiency of nitrate before and after treatment by nanocomposite

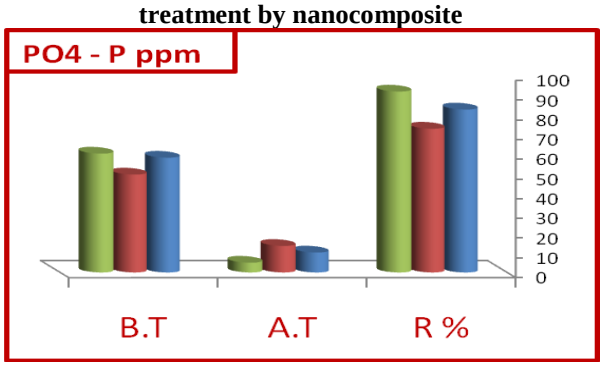

Figure 7. The removal efficiency of phosphate before and after treatment

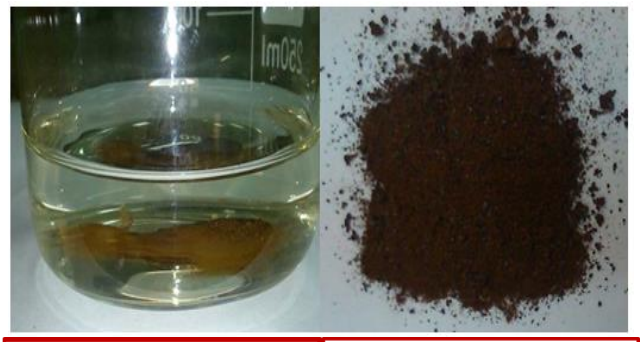

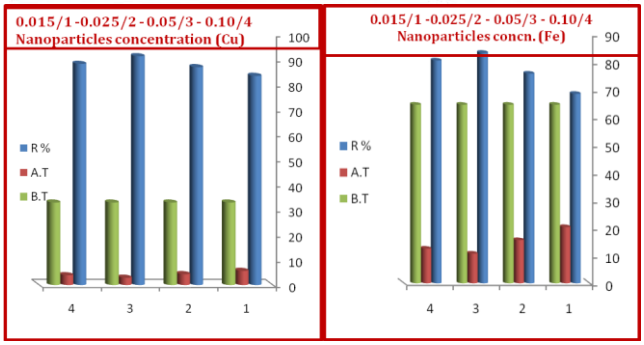

Figure 8. The relation between nanoparticles concentration and reduction percent of Cu & Fe removal/ B.T: Before treatment; A.T: After treatment; R: Reduction%.

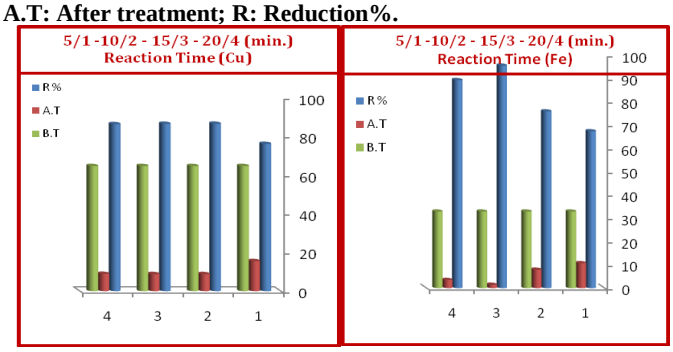

Figure 9. The relation between reaction time and reduction percent of Cu & Fe removal

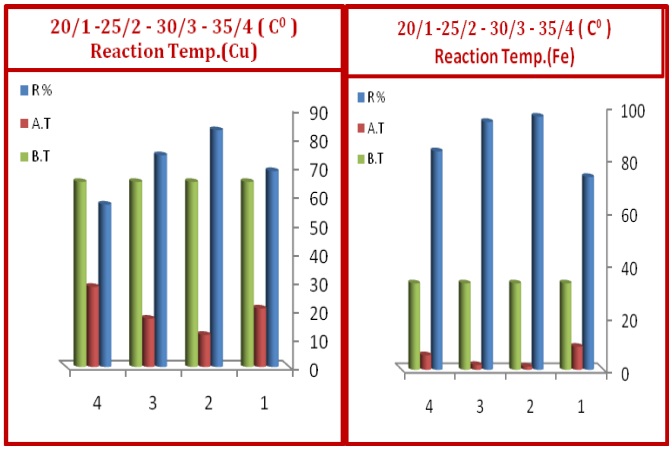

Figure 10. The relation between reaction temperature and reduction percent of Cu & Fe removal

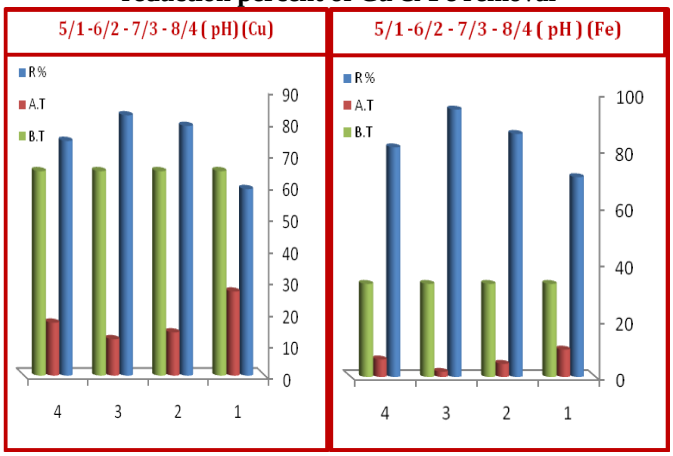

Figure 11. The relation between pH and reduction percent for removal of Cu and Fe ions Optimal condition: Nanoparticles conc. 0.05 g/50ml sonicated for 10 min. at PH 7 and 25 ^{0}C (33)

4. Conclusion

The presence of cellulose acetate with iron oxide nanoparticles gave the nano composite with different characterization and application. The removal efficiency of heavy metals in wastewater increased by using iron oxide/cellulose acetate nanocomposite because the iron oxide nanoparticles insert to the cross linking fibers of cellulose acetate. The new prepared cellulose/iron oxide nanocomposite had new physical and chemical characterization by new additives methodology that had high removal efficiency of heavy metals, nitrates and phosphates upon 86-92 % of inorganic pollutants. This research concerned with copper and iron removal from wastewater using magnetic nanoparticles of cellulose/iron oxide. These results was considered as good yield to treat wastewater of 6 October wastewater station and this technology could be used to reuse polluted water and used as irrigation water in Egypt. The characterization analysis by different instruments showed that cellulose/ iron oxide was in the nano-sized range. Presence of iron oxide nanoparticles gave the nanocomposite more dispersion efficiency and good bio-adsorbent. The saturation magnetization of the iron nano-composite was proportional to the particle size. The adsorption process is a function of pH, reaction time, adsorbent concentration and temperature.

References

[1]L.Fu, V.P.Daravid and D.L.Johnson, "Self-assembled (SA) bilayer molecular coating on magnetic nanoparticles," J. Appl. Surf. Sci., vol. 181, 2001, pp. 173–178.

[2]K.Khalantari, M.B. Ahmad, K.Shameli and R Khandanlou, "Synthesis of talc/Fe_3O_4 magnetic nanocomposites using chemical co-precipitation method," Int. J. Nanomed., vol. 8, 2013, pp. 1–7.

[3]J.L.Zhang, R.S.Srivastava and R.D.K.Misra, "Core-shell magnetite nanoparticles surface encapsulated with smart stimuli-responsive polymer: synthesis, characterization, and last of viable drug-targeting delivery system," Langmuir, vol. 23, 2007, pp. 6342–6351.

[4]Q.Yuan, R Venkatasubramanian, S.Hein and R.D.K. Misra, "A stimulus-responsive magnetic nanoparticle drug carrier: Magnetite encapsulated by chitosan-grafted-copolymer," Acta Biomaterialia, vol. 4, 2008, pp. 1024–1037.

[5]R.D.K.Misra, "Magnetic nanoparticle carrier for targeted drug delivery: perspective, outlook and design," Mater. Sci. Technol., vol. 24, 2008, pp. 1011–1019.

[6]N.J.Tang, W. Zhong, X.L.Wu, H.Y. Jiang, W.Liu and Y.W.Du, "Nanostructured magnetite (Fe_3O_4) thin films prepared by sol-gel method," J. Magn. Magn. Mater., vol. 282, 2004, pp. 92–95.

[7]K.R.Vijaya, Y.Koltypin, Y.S.Cohen, Y.Cohen, D. Aurbach, O.Palchik, I.Felner and A.Gedanken, "Preparation of amorphous magnetite nanoparticles embedded in polyvinyl alcohol using ultrasound radiation," J. Mater. Chem., vol. 10, 2000, pp. 1125–1129.

[8]I. Martinez-Mera, M.E. Espinosa-Pesqueira, R. Pérez-Hernández and J. Arenas-Alatorre, "Synthesis of magnetite (Fe_3O_4) nanoparticles without surfactants at room temperature," Mater. Lett., vol. 61, 2007, pp. 4447–4451.

[9]N.Pinna, S.Grancharov, P.Beato, P. Bonville, M. Antonietti and M. Niedereberger, "Magnetite nanocrystals: Nonaqueous synthesis, characterization and solubility," Chem. Mater., vol. 17, 2005, pp. 3044–3049.

[10]W.S.Chiu, S.Radiman, M.H.Abdullah, P.S.Khiew, N.M.Huang, R.Abd-Shukor, "One pot synthesis of monodisperse Fe_3O_4 nanocrystals by pyrolysis reaction of organometallic compound," Mater. Chem. Phys., vol. 106, 2007, pp. 231–235.

[11]E.Karaoglu, A.Baykal, H.Erdemi, L.Alpsoy and H.Sozeri, "Synthesis and characterization of DL-thioctic acid (DLTA)–Fe_3O_4 nanocomposite," J. Alloys. Compd., vol. 509, 2011, pp. 9218–9225.

[12]B.Unal, M.S.Toprak, Z.Durmus, H.Sözeri and A Baykal, "Synthesis, structural and conductivity characterization of alginic acid–Fe_3O_4 nanocomposite," J. Naopart. Res., vol. 12, 2010, pp. 3039–3048.

[13]J.Singh, P.Kalita, M.K.Singh and B.D.Malhotra, "Nanostructured nickel oxide-chitosan film for application to cholesterol sensor," Applied Physics Letters, vol. 98, 2011, pp. 123702–123704.

[14]J.Singh, M.Srivastava, J.Dutta and P.K.Dutta, "Preparation and properties of hybrid mono-dispersed magnetic α-Fe_2O_3based chitosan nanocomposite film for industrial and biomedical applications," International Journal of Biological Macromolecules, vol. 48, no. 1, 2011, pp. 170–176.

[15] H.L.Liu, S.P.Ko, J.H.Wu, M.H.Jung, J.H.Min and J.H. Lee, "One-pot polyol synthesis of monosize PVP-coated sub-5 nm Fe_3O_4 nanoparticles for biomedical applications," Journal of Magnetism and Magnetic Materials, vol. 310, no. 2, 2007, pp. 815–817.

[16]G.Li, Y.Jiang, K.Huang, P.Ding and J.Chen, "Preparation and properties of magnetic Fe_3O_4–chitosan nanoparticles," Journal of Alloys and Compounds, vol. 466, no. 1–2, 2008, pp. 451–456.

[17]S. ang, H.Bao, P.Yang and G.Chen, "Immobilization of trypsin in polyaniline coated nano-Fe_3O_4/carbon nanotube composite for protein digestion," Analytica Chimica Acta, vol. 612, no. 2, 2008, pp. 182–189.

[18]C. Zhang, J. Shi, X. Yang, L. De and X. Wang, "Effects of calcination temperature and solution pH value on the structural and magnetic properties of $Ba_2Co_2Fe_{12}O_{22}$ferrite via EDTA-complexing process," Materials Chemistry and Physics, vol. 123, no. 2-3, 2010, pp. 551–556.

[19]S.Wang, Y.Tan, D.Zhao and G.Liu, "Amperometric tyrosinase biosensor based on Fe_3O_4 nanoparticles–chitosan nanocomposite," Biosensors and Bioelectronics, vol. 23, no. 12, 2008, pp. 1781–1787.

[20]Y. L. Luo, L.H. Fan, F. Xu, Y. S. Chen, C.H. Zhang and Q.B. Wei, "Synthesis and characterization of Fe_3O_4/PPy/P (MAA-co-AAm) trilayered composite microspheres with electric, magnetic and pH response characteristics," Materials Chemistry and Physics, vol. 120, no. 23, 2010, pp. 590–597.

[21]T.Y. Liu, S.H. Hu, K.H. Liu, D.M. Liu and S.Y. Chen, "Study on controlled drug permeation of magnetic-sensitive ferro gels: Effect of Fe_3O_4 and PVA," Journal of Controlled Release, vol. 126, no. 3, 2008, pp. 228–236.

[22]Q. Xiao, X. Tan, L. Ji and J. Xue, "Preparation and characterization of polyaniline/nano-Fe_3O_4 composites via a novel Pickering emulsion route. Synthetic Metals, vol. 157, no. 18–20, 2007, pp. 784–791.

[23]T. Yang, R.N.C. Brown, L.C., Kempel and P. Kofinas, "Magneto-dielectric properties of polymer
–Fe_3O_4 nanocomposites," Journal of Magnetism and Magnetic Materials, vol. 320, no. 21, 2008, pp. 2714–2720.

[24]H. Sun, X. Zhu, L. Zhang, Y. Zhang and D. Wang, "Capture and release of genomic DNA by PEI modified Fe_3O_4/Au nanoparticles," Materials Science and Engineering C, vol. 30, no. 2, 2010, pp. 311–315.

[25]B.Unal, M.S.Toprak, Z.Durmus, H.Sozeri and A.Baykal, "Synthesis, structural and conductivity characterization of alginic acid-Fe_3O_4 nanocomposite," Journal of Nano-particle Research, vol. 12, no. 8, 2010, pp. 3039–3048.

[26]C. Zhang, J. Shi, X. Yang, L. De and X. Wang, "Effects of calcination temperature and solution pH value on the structural and magnetic properties of $Ba_2Co_2Fe_{12}O_{22}$ ferrite via EDTA-complexing process. Materials Chemistry and Physics, vol. 123, no. 2-3, 2010, pp. 551–556.

[27]Y.F. Shen, J. Tang, Z.H. Nie, Y.D. Wang, Y. Ren and L. Zuo, "Preparation and application of magnetic Fe_3O_4 nanoparticles for wastewater purification," Sep. Purif. Technol., vol 68, 2009, pp. 312–319.

[28]M.Mahdavi, M.B.Ahmad, M.J.Haron, Y.Gharayebi, K. Shameli and B. Nadi, "Fabrication and characterization of SiO_2/(3-Aminopropyl) triethoxysilane-coated magnetite nanoparticles for Lead (II) removal from aqueous solution," J. Inorg. Organ met. Polym., vol. 23, 2013, pp. 599–607.

[29]B. Bock, F. Karsten, J. Helmut, M. Kuhr and H. Musso, "Bond character of beta diketone metal chelates," Angewandte Chemie International Edition, vol. 10, nol. 4, 1971, pp. 225.

[30]W.A.Hosny, H. El- Saied and A.H. Basta, "Metal Chelates with Some Cellulose Derivatives: V. Synthesis and Characterization of some Iron (III) Complexes with Cellulose Ethers," Polymer International., vol. 42, 1997, pp. 157-162.

[31]M. Mahdavi, F. Namvar, M.B. Ahmad and R. Mohamad, "Green biosynthesis and characterization of magnetic iron oxide (Fe_3O_4) nanoparticles using seaweed (Sargassum muticum) aqueous extract," Moecules, vol. 18, 2007, pp. 5954–596.

[32]L. Guo, G. Liu, R.Y. Hong and H.Z. Li, "Preparation and characterization of chitosan poly (acrylic acid) magnetic microspheres," Marine Drugs, vol. 8, 2010, pp. 2212–2222.

[33]Magdy.H.El-Sayed and Yasser A.M. Abdulhady. "Heavy metals removal by using magnetic iron oxide/TiO_2 nanocomposite for wastewater treatment in 10^{th} of Ramadan city, Egypt". Egyptian J. Desert Res., **65**, No. 1, (2015)81-99.